

## Ion-Molecule Reactions in the Binary Mixture of Ethylene Oxide and Trioxane. I. Hydrogen Atom and Proton Transfer Reactions

Minoru KUMAKURA and Toshio SUGIURA\*

*Takasaki Radiation Chemistry Research Establishment, Japan Atomic Energy Research Institute, Takasaki, Gunma 370-12*

*\*Japan Atomic Energy Research Institute, Shinbashi, Minato-ku, Tokyo 105*

(Received December 13, 1976)

The formation mechanism of protonated molecular ions by cross-reactions in ethylene oxide–trioxane mixtures has been studied with use of a modified time-of-flight mass spectrometer. The precursors of the product ions were determined by analysis of the fine structure of their ionization efficiency curves using deuterated ethylene oxide. Protonated ethylene oxide is formed by the hydrogen atom transfer reaction of ethylene oxide molecular ion with trioxane, and protonated trioxane by the proton transfer reaction of  $\text{CHO}^+$  (from ethylene oxide) with trioxane. In the ion-molecule reactions of ethylene- $d_4$  oxide–trioxane mixtures, appreciable isotope effect was observed. The  $\text{CHO}^+$  from ethylene oxide is an important reactant ion as compared with that from trioxane in the proton transfer reaction, and  $\text{CHO}^+$  from ethylene oxide was suggested as a thermal reactive ion. The order of proton affinity could be estimated from the proton transfer reactions involving  $\text{CHO}^+$ . It was found that the proton affinity of trioxane is smaller than that of ethylene oxide.

The ion-molecule reactions in trioxane (1,3,5-trioxane) and ethylene oxide have been studied in connection with an elementary process in radiation and ion chemistry.<sup>1,2</sup> In trioxane, consecutive-association reactions of protonated ions with trioxane were observed, but the reactions were not carried out in ethylene oxide. The results of the ion-molecule reactions could be correlated with the behavior of observed radiation-induced polymerization in which trioxane was easily polymerized,<sup>3,4</sup> appreciable polymerization taking place less easily in ethylene oxide.<sup>5</sup> On the other hand, protonated ethylene oxide was mainly formed by the proton transfer reaction from  $\text{CHO}^+$  in ethylene oxide,  $\text{CHO}^+$  from trioxane not playing an important role for the formation reaction of protonated trioxane.<sup>1</sup> It seems that the reactivity of  $\text{CHO}^+$  in proton transfer reaction is attributed to the molecular source producing  $\text{CHO}^+$ . The proton transfer reaction due to  $\text{CHO}^+$  would be affected by the property of neutral molecule. Futrell *et al.*<sup>6</sup> studied the effect of the kinetic energy of  $\text{CHO}^+$  in proton transfer reactions with a tandem mass spectrometer, and stated that the reactivity of  $\text{CHO}^+$  is affected by its energy state. Various oxygenated fragment ions are produced by electron impact from compounds containing oxygen. Since oxygenated ions giving the same structure are produced from various cyclic ether, it is of interest to examine the reactivity of these ions. The formation reaction of protonated molecular ions has been studied for alcohols,<sup>7–9</sup> ketones,<sup>10–12</sup> aldehydes,<sup>11–13</sup> and dimethyl ether,<sup>11,12</sup> but not for cyclic compounds containing oxygen. The ion-molecule reactions in pure system of ethylene oxide and trioxane have been studied.<sup>1,2</sup> The present work deals with the formation mechanism of the protonated molecular ions by cross-reactions (reactions between ions of one molecule and the molecules of the other) in ethylene oxide (or ethylene- $d_4$  oxide)–trioxane mixtures. The reactivity of the  $\text{CHO}^+$  ions from both ethylene oxide and trioxane was examined by means of proton transfer reactions.

### Experimental

A Bendix Model 12-101 time-of-flight mass spectrometer was used. A part of the spectrometer was modified in order to study ion-molecule reactions.<sup>2</sup> Some pulse electronic circuits of the apparatus were modified. A Hewlett Packard 214A pulse generator and a pulse generator (Sanwa Denshi Production Co., Ltd.) were used for supplying the ionizing and ion withdrawal pulses. A variable delay time circuit permitted a variation of the time between the end of the ionizing pulse and the onset of the ion withdrawal pulse.<sup>2</sup> During the delay time, the entire ionization chamber is field-free, so that ion-molecule reactions occurring during the time interval are under purely thermal conditions.

The retarding potential differential technique (RPD) was adopted for appearance potential and ionization efficiency curve measurement. A report has been given on the technique.<sup>14</sup> The measurement of the ionization efficiency curves of two ions was simultaneously performed by the two-channel ion detection method. The ion currents of two different ions were recorded with a Rikadenki R-34 three-pen recorder.

The gas-sample inlet-system consisting of a dual-leak and dual-reservoir was used. Two kinds of samples are introduced individually into the ionization chamber through two separate leaks from separate reservoirs (5L). The partial pressure of the two samples was indirectly measured with an MKS Baratron 90-X RP-2 capacitance manometer and the pressure was calibrated by known rate constant ( $1.11 \times 10^{-9} \text{ cm}^3 \text{ molecule}^{-1} \text{ s}^{-1}$ ) of  $\text{CH}_5^+$  in the ion-molecule reaction of methane.<sup>15</sup>

The following reagents were used: trioxane (Celanese Chemical), ethylene oxide (Nisso Yuka Industry Co., Ltd.), and ethylene- $d_4$  oxide (Merck Sharp and Dohme of Canada, deuterium atom purity, least 98%). The samples were used after being subjected to vacuum distillation several times.

### Results and Discussion

**Delay Time Dependence.** The delay time dependence plots of fragment ions in a 1:1 mixture of ethylene oxide and trioxane are shown in Fig. 1. The plots were obtained as a function of delay time at ionization chamber pressure of  $1.70 \times 10^{13} \text{ molecules cm}^{-3}$ . The  $m/e$  44 ( $\text{C}_2\text{H}_4\text{O}^+$ ), 43 ( $\text{C}_2\text{H}_3\text{O}^+$ ), and 29 ( $\text{CHO}^+$ ) are

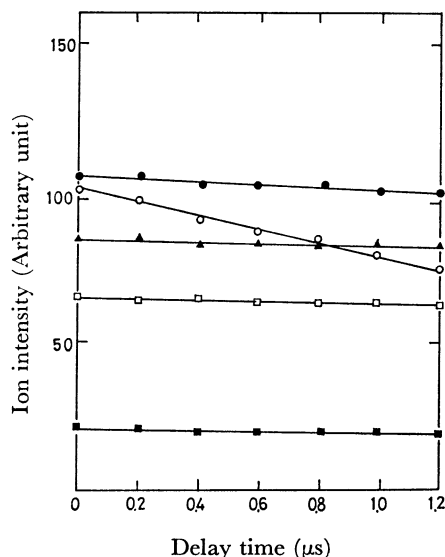


Fig. 1. Delay time dependence of fragment ions in ethylene oxide–trioxane mixtures.

●:  $C_2H_5O_2^+$ , ▲:  $C_2H_4O^+$ , ●:  $CHO^+ (\times 1/2)$ ,  
□:  $C_3H_5O_3^+$ , ■:  $C_2H_3O^+$ .

major fragment ions from ethylene oxide, while  $m/e$  89 ( $C_3H_5O_3^+$ ), 61 ( $C_2H_5O_2^+$ ), and a part of  $m/e$  29 are those from trioxane.

The delay time dependence plots of product ions are shown in Fig. 2. The formation of protonated ethylene oxide ( $m/e$  45,  $C_2H_5O^+$ ) is remarkable as compared with protonated trioxane ( $m/e$  91,  $C_3H_7O_3^+$ ), the ion intensity ratio of  $C_2H_5O^+$  to  $C_3H_7O_3^+$  being *ca.* 5.5 at delay time of 1.0  $\mu s$ .

The ion-molecule reactions in ethylene- $d_4$  oxide–trioxane mixtures were studied in order to clarify the formation mechanism of product ions under the same conditions as for ethylene oxide–trioxane mixtures. The plots of delay time dependence for fragment and isotopic product ions are shown in Figs. 3 and 4, respectively.

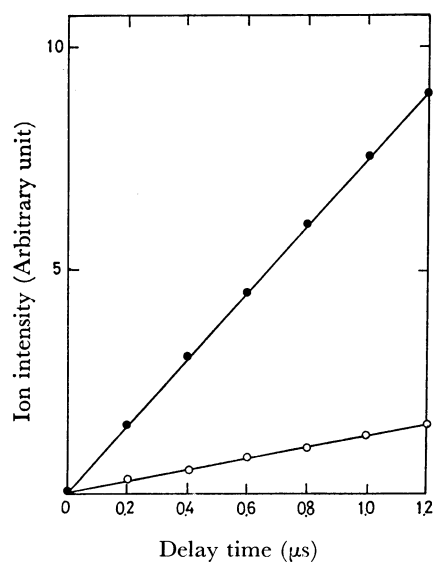


Fig. 2. Delay time dependence of protonated molecular ions in ethylene oxide–trioxane mixtures.

●:  $C_2H_5O^+$ , ○:  $C_3H_7O_3^+$ .

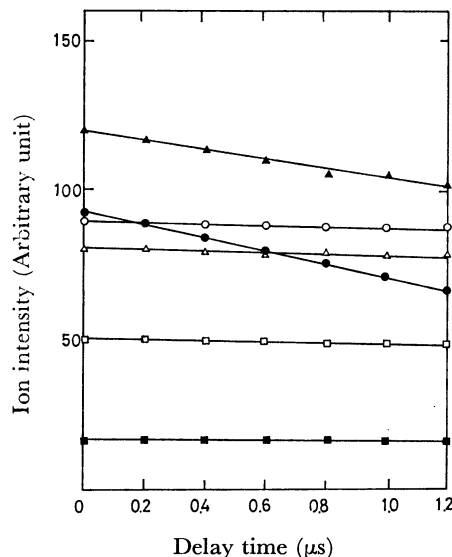


Fig. 3. Delay time dependence of fragment ions in ethylene- $d_4$  oxide–trioxane mixtures.

▲:  $CDO^+ (\times 1/2)$ , ○:  $C_2H_5O_2^+$ , △:  $C_2D_4O^+$ ,  
□:  $C_3H_5O_3^+$ , ●:  $CHO^+ (\times 1/2)$ , ■:  $C_2H_3O^+$ .

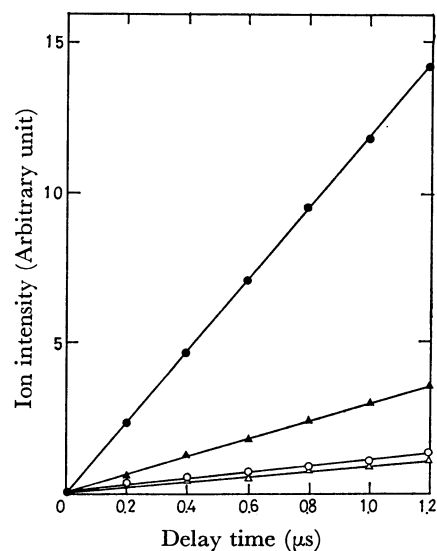


Fig. 4. Delay time dependence of protonated and deuterated molecular ions in ethylene- $d_4$  oxide–trioxane mixtures.

●:  $C_2D_4HO^+ (\times 2)$ , ▲:  $C_2D_5O^+ (\times 2)$ , ○:  $C_3H_7O_3^+$ ,  
△:  $C_3H_6DO_3^+ (\times 5)$ .

The  $CHO^+$  ions from both molecules are separated into  $CHO^+$  and  $CDO^+$ . The ions markedly decreased with increasing delay time as compared with other fragment ions of high mass number (Fig. 3). The cause of decrease is mainly due to a mass discrimination effect though there is a contribution of these ions to ion-molecule reactions. The isotopic distribution of product ions is given in Fig. 4. The  $m/e$  49 ( $C_2D_4HO^+$ ) and 50 ( $C_2D_5O^+$ ) are protonated and deuterated trioxane, respectively. The  $C_2D_4HO^+$  and  $C_3H_6DO_3^+$  ions are formed by cross-reactions and the  $C_2D_5O^+$  and  $C_3H_7O_3^+$  ions by homo-reactions. The ion intensity ratios of  $C_2D_4HO^+$  to  $C_2D_5O^+$ , and  $C_3H_6DO_3^+$  to  $C_3H_7O_3^+$

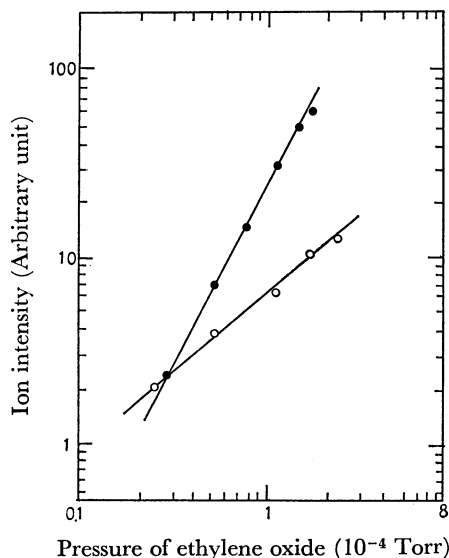


Fig. 5. Pressure dependence of protonated molecular ions to ethylene oxide at delay time of 1.0  $\mu$ s.

●:  $\text{C}_2\text{H}_5\text{O}^+$ , ○:  $\text{C}_3\text{H}_7\text{O}_3^+$ .

$\text{O}_3^+$  are *ca.* 5 and 0.2 at delay time of 1.0  $\mu$ s, suggesting that a drastic reaction occurs in the mixture system.

**Pressure Dependence.** The pressure dependence of the product ions on each molecule was examined in order to clarify the contribution of molecules of ethylene oxide and trioxane. The pressure dependence plots of the protonated molecular ions on the pressure of ethylene oxide, shown in Fig. 5, were obtained by the pressure variation of ethylene oxide at fixed pressure ( $8.5 \times 10^{12}$  molecules  $\text{cm}^{-3}$ ) of trioxane and delay time of 1.0  $\mu$ s. Protonated ethylene oxide shows a dependence of *ca.* second order on the pressure of ethylene oxide, while protonated trioxane shows one of *ca.* first order. This suggests that the formation of protonated trioxane is correlated with ethylene oxide.

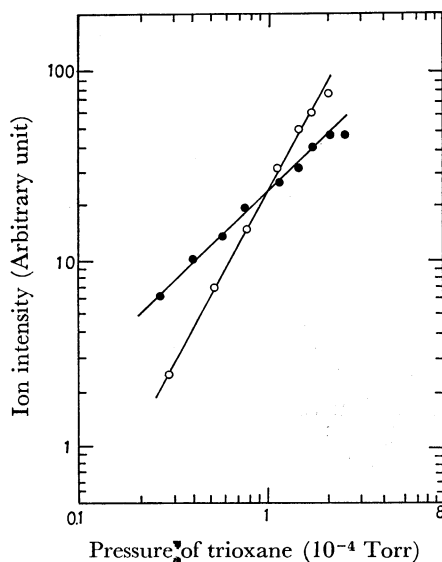


Fig. 6. Pressure dependence of protonated molecular ions to trioxane at delay time of 1.0  $\mu$ s.

●:  $\text{C}_2\text{H}_5\text{O}^+$ , ○:  $\text{C}_3\text{H}_7\text{O}_3^+$ .

The pressure dependence plots of protonated molecular ions to trioxane at fixed pressure ( $8.5 \times 10^{12}$  molecules  $\text{cm}^{-3}$ ) of ethylene oxide are shown in Fig. 6. Protonated trioxane shows the dependence of second order on trioxane pressure and protonated ethylene oxide that of the first order on trioxane one. These results suggest that protonated ethylene oxide and trioxane are formed by means of proton or hydrogen atom transfer reactions.

**Ionization Efficiency Curves.** The ionization efficiency curves of fragment and product ions in ethylene- $d_4$  oxide-trioxane mixtures were measured at delay time of 1.0  $\mu$ s. The ionization efficiency curves of  $\text{C}_2\text{D}_4\text{HO}^+$ ,  $\text{C}_2\text{D}_4\text{O}^+$ , and  $\text{C}_3\text{H}_5\text{O}_3^+$  are shown in Fig. 7, and those of  $\text{C}_3\text{H}_6\text{DO}_3^+$ ,  $\text{C}_2\text{D}_5\text{O}^+$ , and  $\text{CDO}^+$  in Fig. 8. The precursors of the product ions can be identified by comparison of the onset and fine structures of the curves of these product ions with those of fragment ions.

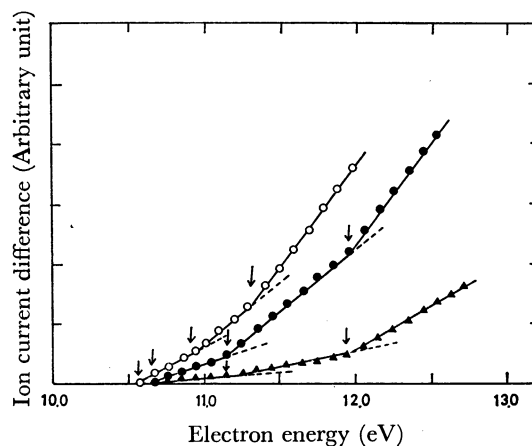


Fig. 7. Ionization efficiency curves of  $\text{C}_2\text{D}_4\text{O}^+$  (●),  $\text{C}_2\text{D}_4\text{HO}^+$  (▲), and  $\text{C}_3\text{H}_5\text{O}_3^+$  (○) in ethylene- $d_4$  oxide-trioxane mixtures.

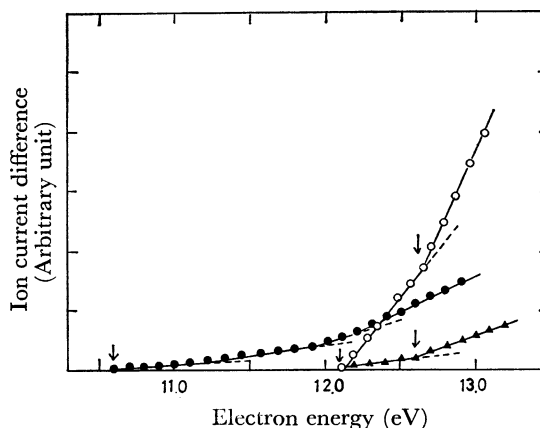


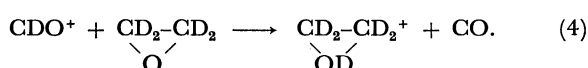
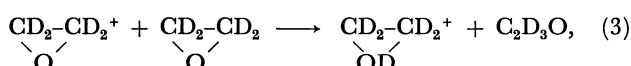
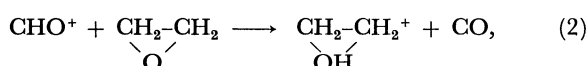
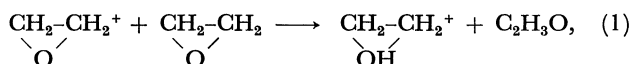
Fig. 8. Ionization efficiency curves of  $\text{CDO}^+$  (○),  $\text{C}_2\text{D}_5\text{O}^+$  (●), and  $\text{C}_3\text{H}_6\text{DO}_3^+$  (▲) in ethylene- $d_4$  oxide-trioxane mixtures.

The ionization potential of ethylene oxide and the appearance potential of  $\text{C}_3\text{H}_5\text{O}_3^+$  from trioxane were  $10.64 \pm 0.1$  and  $10.59 \pm 0.05$  eV, respectively.<sup>2,14</sup> The onset and break points in the ionization efficiency curves of both  $\text{C}_2\text{D}_4\text{HO}^+$  and  $\text{C}_2\text{D}_4\text{O}^+$  agree. The onset of

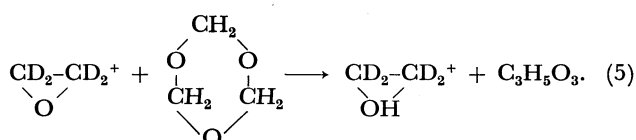
$C_2D_4HO^+$  approached that of  $C_3H_5O_3^+$ ; however, the fine structures of both curves differ from each other. The appearance potential of other fragment ions from trioxane is higher than that of  $C_2D_4HO^+$ .<sup>14</sup> The break points of the curve of  $C_2D_4HO^+$  does not agree with the appearance potentials of these fragment ions. It is concluded that the precursor of  $C_2D_4HO^+$  is  $C_2D_4O^+$  and fragment ions from trioxane does not correlate as a precursor.

The onset of  $C_3H_6DO_3^+$  agrees with that of  $CDO^+$  and is higher than the ionization potential of  $C_2D_4O^+$  by *ca.* 1.5 eV. The fine structures of the ionization efficiency curves of  $C_3H_6DO_3^+$  and  $C_2D_4O^+$  differ from each other. The appearance potentials of other fragment ions from ethylene oxide deviate from that of  $C_3H_6DO_3^+$ , and thus these ions do not contribute to the formation of  $C_3H_6DO_3^+$ . From the results, we see that the precursor of  $C_3H_6DO_3^+$  is  $CDO^+$  from ethylene- $d_4$  oxide.

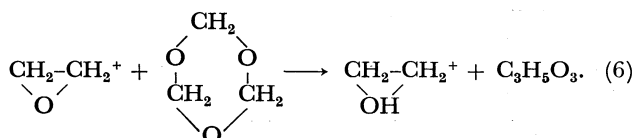
**Reaction Mechanism.** It is found that a part of  $C_2H_5O^+$  and  $C_2D_5O^+$  is formed by the following reactions in ethylene oxide (or ethylene- $d_4$  oxide)–trioxane mixtures, as observed in the ion-molecule reactions in pure ethylene oxide.<sup>2)</sup>



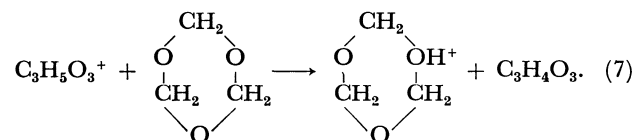
The ion intensity of  $C_2D_4HO^+$  increases with increasing delay time (Fig. 4), and the appearance potential of this ion agrees with the ionization potential of ethylene- $d_4$  oxide (Fig. 7). Thus, it is suggested that  $C_2D_4HO^+$  is formed by hydrogen atom transfer reaction as follows.



This shows that predominant formation of  $C_2H_5O^+$  in ethylene oxide–trioxane mixtures is due to Reaction 6 rather than Reactions 1 and 2.

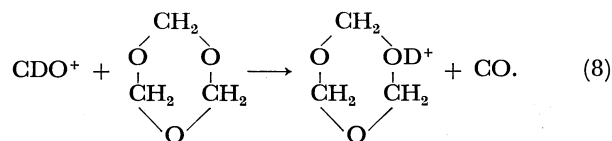


$C_3H_7O_3^+$  was formed by Reaction 7 in ion-molecule reactions of trioxane.<sup>1)</sup>

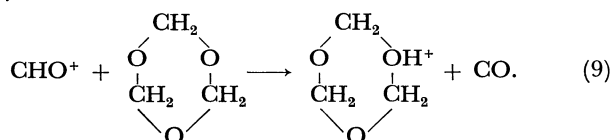


It was observed that the ion intensity of  $C_3H_6DO_3^+$  increases slightly with increasing delay time in ethylene-

$d_4$  oxide–trioxane mixtures (Fig. 4). From the ionization efficiency curves (Figs. 7 and 8), it is concluded that  $C_3H_6DO_3^+$  in ethylene- $d_4$  oxide–trioxane mixtures is formed by deuteron transfer from  $CDO^+$  to trioxane molecule.



In the ion-molecule reactions of ethylene oxide,  $\text{CHO}^+$  was an important reactant ion in the formation reaction of protonated ethylene oxide.<sup>2)</sup>  $\text{CHO}^+$  is a proton donor ion. It follows that Reaction 8 predominates in the formation of  $C_3H_6DO_3^+$ . Similarly, Reaction 9 would participate in the formation of  $C_3H_7O_3^+$  in ethylene oxide–trioxane mixtures.



**Rate Constants.** In the calculation of the rate constant for  $C_2H_5O^+$  formed in the mixture system, the ion intensities of  $C_2H_4O^+$  and  $C_2H_5O^+$  are corrected. The equation of rate constant ( $k_6$ ) for Reaction 6 can be expressed as follows:

$$\frac{I_{C_2H_5O^+(M)} - I_{C_2H_5O^+(E)}}{I_{C_2H_4O^+(M)}} = k_6 [C_3H_6O_3] t + C, \quad (10)$$

where  $I_{C_2H_5O^+(M)}$  and  $I_{C_2H_4O^+(M)}$  are the ion intensities of  $C_2H_5O^+$  and  $C_2H_4O^+$  in ethylene oxide–trioxane mixtures, respectively;  $I_{C_2H_5O^+(E)}$  is the ion intensity of  $C_2H_5O^+$  formed in the ion-molecule reactions of pure ethylene oxide;<sup>2)</sup>  $[C_3H_6O_3]$  is the concentration of trioxane in the ionization chamber, and  $t$  is delay time. The rate constants obtained are given in Table 1. The rate constants of the formation reactions of protonated and deuterated molecular ions in ethylene oxide (or ethylene- $d_4$  oxide)–trioxane mixtures are summarized in Table 1.

TABLE 1. RATE CONSTANTS

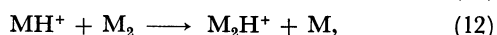
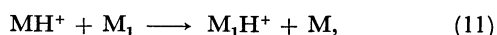
Ethylene oxide–trioxane		Ethylene- $d_4$ oxide–trioxane	
Reaction	$k \times 10^9$ cm <sup>3</sup> molecule <sup>-1</sup> s <sup>-1</sup>	Reaction	$k \times 10^9$ cm <sup>3</sup> molecule <sup>-1</sup> s <sup>-1</sup>
(1)	0.145 <sup>a)</sup>	(3)	0.130
(2)	2.09 <sup>a)</sup>	(4)	1.81
(6)	4.00	(5)	4.18
(7)	1.15 <sup>a)</sup>	(7)	1.10
(9)	0.121	(8)	0.101

a) Ref. 2.

**Reactivity.** The molecular ion from trioxane is unstable. Its ion intensity is relatively low, while that from ethylene oxide is high (Fig. 1). Thus, the reactivity of molecular ion from trioxane can not be discussed in comparison with that from ethylene oxide. On the other hand, it is of interest to examine the reactivity of the  $\text{CHO}^+$  ions from both molecules. The  $\text{CHO}^+$  from ethylene oxide participates preferentially for

proton transfer reaction as compared with that from trioxane in the mixture system. No contribution of  $\text{CHO}^+$  for protonated trioxane has been observed in the ion-molecule reactions of trioxane.<sup>1)</sup> A proton transfer reaction involving  $\text{CHO}^+$  seems to be affected by its energy state. It was demonstrated that the energy of  $\text{CHO}^+$  from trioxane is considerably higher than that of ethylene oxide in the measurement of the translational energies of the  $\text{CHO}^+$  ions from oxygen-containing organic compounds.<sup>16)</sup> It is suggested that  $\text{CHO}^+$  from ethylene oxide is a thermal reactive ion as compared with that from trioxane.

**Proton Affinity.** The proton affinity of ethylene oxide has been reported to be 183 kcal mol<sup>-1</sup>.<sup>17,18)</sup> The proton affinity of trioxane is not known but the basicities for trioxane and ethylene oxide which correlate with their proton affinities have been found to be 10 and 7.3 respectively.<sup>19)</sup> In this mixture system, the reactant ions in Reactions 2 and 9 are  $\text{CHO}^+$  from ethylene oxide, the rate constant ratio ( $k_2/k_9$ ) being 17.3. This indicates that the proton affinity of ethylene oxide is larger than that of trioxane. The proton affinity of a molecule is defined as the enthalpy change for proton transfer reactions. A number of determinations of absolute proton affinity have been undertaken by the appearance potential method and an empirical correlation of excess energies in ion-molecule reactions.<sup>18)</sup> The relative proton affinity was also studied from observation of ion-molecule reactions.<sup>20-22)</sup> It is found that the order of relative proton affinity can be estimated using rate constant in proton transfer reaction involving  $\text{CHO}^+$ . The general scheme is as follows:



where the order of proton affinity (PA) for neutral molecule ( $\text{M}_1$ ,  $\text{M}_2$ ) is  $\text{PA}(\text{M}_1) > \text{PA}(\text{M}_2)$ , when the rate constant in both reactions is  $k_{11} > k_{12}$ . A proton donor ion such as  $\text{CHO}^+$  which is a thermal energy ion is desirable for reactant ion ( $\text{MH}^+$ ).

**Isotope Effects.** The difference of the rate constant in the proton and deuteron transfer reactions was observed (Table 1). The ratios  $k_1/k_3$ ,  $k_2/k_4$ , and  $k_9/k_8$  were 1.12, 1.15, and 1.20, respectively. The values of  $k_5$  and  $k_6$  were almost equal. Gupta *et al.*<sup>23)</sup> studied the isotope effects in the ion-molecule reactions of water and methane. They reported that the ratio of the rate constant for proton (from  $\text{OH}^+$ ) and deuteron transfer (from  $\text{OD}^+$ ) is 2.10, and the ratio of the rate constant for the formation of  $\text{CH}_5^+$  and  $\text{CD}_5^+$  1.49. Chong and Franklin<sup>24)</sup> observed that the rate constants for the transfer of an H or a D atom are the same, but the rate constant of the transfer of  $\text{D}^+$  is only *ca.* 0.62 times as great as that for an  $\text{H}^+$  in ion-molecule reactions of methane-methane- $d_4$  mixtures. The isotope effect we

observed is smaller than theirs.

The authors wish to express appreciation to Prof. K. Hayashi, Osaka University, and Dr. A. Ito and Mr. K. Arakawa of our Establishment for interesting and stimulating discussions.

## References

- 1) M. Kumakura and T. Sugiura, in "Recent Developments in Mass Spectroscopy," ed by K. Ogata and T. Hayakawa, Univ. of Tokyo Press, Tokyo (1970), p. 988.
- 2) M. Kumakura, A. Ito, and T. Sugiura, *Mass Spectroscopy*, **22**, 61 (1974).
- 3) K. Hayashi, H. Ochi, and S. Okamura, *J. Polym. Sci., Part A-2*, **1964**, 2929.
- 4) M. Sakamoto, I. Ishigaki, M. Kumakura, H. Yamashina, T. Iwai, A. Ito, and K. Hayashi, *J. Macromol. Chem.*, **1**, 639 (1966).
- 5) D. Cordischi, A. Mele, and A. Somogyi, "Proceedings of the Second Tihany Symposium on Radiation Chemistry," ed by J. Dobo and P. Hedvig, Akad. Kiado, Budapest (1967), p. 483.
- 6) J. H. Futrell, F. P. Abramson, A. K. Bhattacharya, and T. O. Tiernan, *J. Chem. Phys.*, **52**, 3655 (1970).
- 7) J. M. S. Henis, *J. Am. Chem. Soc.*, **90**, 1477 (1970).
- 8) K. R. Ryan, L. W. Sieck, and J. H. Futrell, *J. Chem. Phys.*, **41**, 111 (1964).
- 9) S. K. Gupta, E. G. Jones, A. G. Harrison, and J. J. Myher, *Can. J. Chem.*, **45**, 3107 (1967).
- 10) K. A. G. Macneil and J. H. Futrell, *J. Phys. Chem.*, **76**, 409 (1972).
- 11) H. Prichard and A. G. Harrison, *J. Chem. Phys.*, **48**, 5623 (1968).
- 12) A. S. Blair and A. G. Harrison, *Can. J. Chem.*, **51**, 703 (1973).
- 13) S. Okada, A. Matsumoto, T. Dohmaru, S. Taniguchi, and T. Hayakawa, *Mass Spectrosc.*, **20**, 311 (1972).
- 14) M. Kumakura, T. Sugiura, and S. Okamura, *Mass Spectrosc.*, **16**, 16 (1968).
- 15) C. W. Hand and H. Weyssenhoff, *Can. J. Chem.*, **42**, 195 (1964).
- 16) M. Kumakura, K. Arakawa, and T. Sugiura, to be published.
- 17) J. L. Beauchamp and R. C. Dunbar, *J. Am. Chem. Soc.*, **92**, 1477 (1970).
- 18) B. H. A. Haney and J. L. Franklin, *Trans. Faraday Soc.*, **65**, 1794 (1968).
- 19) E. Z. Utyanskaya, *Polym. Sci. USSR*, **13**, 595 (1971).
- 20) V. L. Talroze and E. L. Frankevich, *Dokl. Akad. Nauk SSSR*, **111**, 376 (1956).
- 21) J. L. Beauchamp and S. E. Buttrill, *J. Chem. Phys.*, **48**, 1783 (1968).
- 22) D. Holtz and J. L. Beauchamp, *J. Am. Chem. Soc.*, **91**, 5913 (1969).
- 23) S. K. Gupta, E. G. Jones, A. G. Harrison, and J. J. Myher, *Can. J. Chem.*, **45**, 3107 (1967).
- 24) S. L. Chong and J. L. Franklin, *J. Chem. Phys.*, **55**, 641 (1971).